Numerical simulation and tank tests of the free-floating Sloped IPS buoy

Numerical simulation and tank tests of the free-floating Sloped IPS Buoy

P.Parkin, G.Payne, J.R.M. Taylor
School of Engineering and Electronics, University of Edinburgh

Abstract

Earlier work at the University of Edinburgh showed that the sloped IPS buoy wave energy device had the potential for high power capture across a surprisingly wide range of wave periods. Those results came from tank tests on artificially constrained models with fixed external reaction sources. However the future of the sloped IPS concept depends on the performance of free-floating devices. Accordingly, the wave power group at Edinburgh is now working on realistic models of the sloped IPS buoy using both tank tests and numerical models.

Tank tests and numerical modeling are complementary activities. Tank data is needed to verify the formulation and accuracy of the numerical models. Those models can then be used to illuminate the effects of possible variations in device shapes and power take-off characteristics. Such predictions, being based on linear theory, will usually be restricted to regular, unidirectional waves of relatively small height. However, tank tests can then be used to extend understanding of the behaviour of particular device ideas into simulations of the three-dimensional ocean conditions that will drive the full-scale engineering design.

Numerical modeling was carried out using WAMIT, a hydrodynamics package that is widely used in the offshore industry. The experimental models were tested in the new Edinburgh 'curved' tank. A model consisted of a float, an inertia plate and a self-contained dynamometer tube. Results are presented from tank tests and numerical modeling of the motions of both an artificially constrained and a free floating model sloped IPS buoy.

1. Background to the sloped IPS buoy

The concept of the sloped IPS buoy was first described by Salter and Lin (1995) and is an idea that evolves from the Swedish wave power device, the IPS buoy. The IPS buoy consists of a floating buoy connected to a submerged vertical tube open to the sea at both ends. Inside the tube is a piston which acts as a reaction plate and drives hydraulic rams within the buoy. In waves the buoy heaves in response to the surface and near-surface wave motion whilst the piston remains relatively fixed by its coupling to the more static deep water. The buoy can therefore operate with no reference to the sea-bed. Further reference to the IPS buoy can be found in Fredrikson (1992) and EC Report (1993).

The aim of any wave energy developer is to keep costs as low as possible. One of the factors affecting the cost of a device is the size. In general, the smaller the device, the cheaper it is. Size is generally closely linked to natural frequency and hence to the wavelengths of economic interest for power generation. To reduce the overall size of a buoyant device relative to its design wavelength therefore suggests that its natural frequency should be somehow decreased. The natural frequency of a simple buoyant device is directly proportional to the square root of its hydrostatic stiffness (due to buoyancy) and inversely proportional to the square root of its mass (including added virtual mass). So, on the basis that increasing the mass is not likely to make the device cheaper, the most promising route to reduce natural frequency and hence device size is by finding a way to reduce the stiffness due to buoyancy. Purely heaving devices tend to have high but narrow frequency bands at relatively short periods. One the other hand, purely surging devices, such as the Mace (Salter, 1992), tend to have natural resonance periods longer than the useful parts of the wave spectrum, giving them low energy productivity. If the natural period of heaving buoys are too short and those of surging devices too long, then it may follow that intermediate angles of motion could have mid-range resonance periods. This idea was supported by a generic numerical study by Pizer (1994) of a range of hemispheres and ellipsoids moving at different angles to the oncoming wave. His predictions showed that for two identical hemispheres, one moving vertically and the other moving at 30° to the horizontal, both with plain damping, the productivity of the sloped configuration was far superior, despite it having lower forces. Furthermore, by changing the slope angle from 30° to 45° the resonance shifted from 11 to 8 seconds. Thus a device could be tuned by active slope angle control.

The sloped IPS buoy (see Figure 1) combines desirable features of the IPS with the idea of angled movement. The slope constraint would be achieved by enclosing a number of IPS power take off tubes in a wide planar construction so the device would have large added mass in the direction perpendicular to the slope but retain the hydrodynamics of a smaller buoy in the parallel direction.

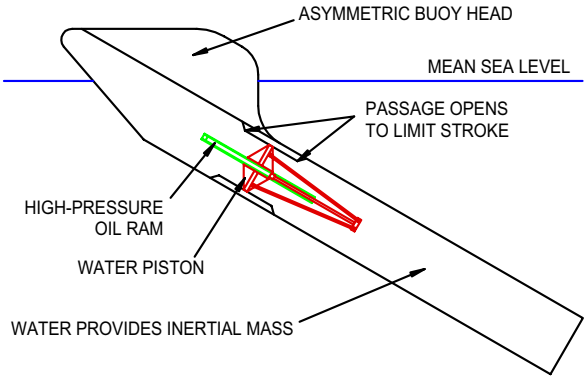

Figure 1: *Cross-section of the conceptual sloped IPS buoy and one of its water tubes. Waves approach from the right.*

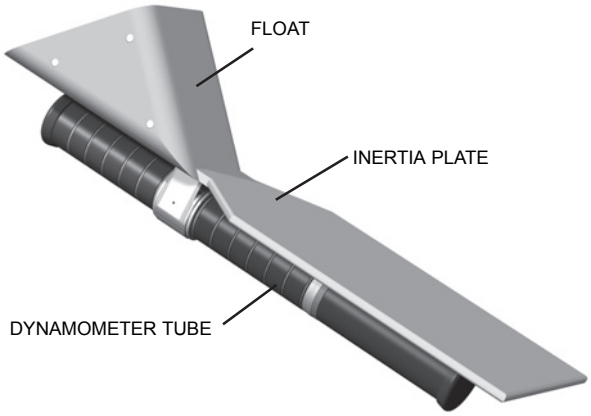

Figure 2: *The components of a typical free floating experimental model.*

2. Introduction to the present work

Initial tank measurements of the sloped IPS buoy concept were carried out by Lin (Salter and Lin, 1998, Lin, 1999). These used artificially constrained semi-circular models with fixed external reaction sources. The results showed the effect of slope to be as hoped for, with high power capture across a surprisingly wide range of wave periods. The future of the sloped IPS buoy, however, depends on the performance of free-floating devices, so the wave power group at Edinburgh is now working on more realistic models.

The jump from a constrained model with an external reaction source to a fully free-floating device with an internal reaction source is a large one. Accordingly, two intermediate steps are being investigated. The first of these is to make the move from an external reaction source to an internal reaction source whilst continuing to *artificially constrain* the model to move in the desired direction (constrained free-floating model). The second is to remove all restraint so that the model is freely floating (fully free-floating model), but only to study the *movement* of the model with different tube and plate configurations.

As tools of investigation, both numerical modelling and tank tests have been used. The tank data was used to verify the formulation and accuracy of the numerical models, which could then be used to illuminate the effects of possible variations in device configuration. This paper describes results from the following:

- Comparison of numerical simulations with historic experimental data.
- Experimental measurement of the motions of a constrained free-floating model.
- Experimental measurements and numerical predictions of the motions of a fully free-floating model.
- Motions of a free-floating model with a different inertia plate, measured experimentally.

3. Experimental models

The physical models typically consist of a float, an inertia plate and a self-contained dynamometer tube (see Figure 2). The dynamometer is able to absorb power from the float motion by reacting it against the mass of water contained within its tube. The development of the dynamometer tube formed the first part of the current work and is described in detail in Taylor and Mackay (2000).

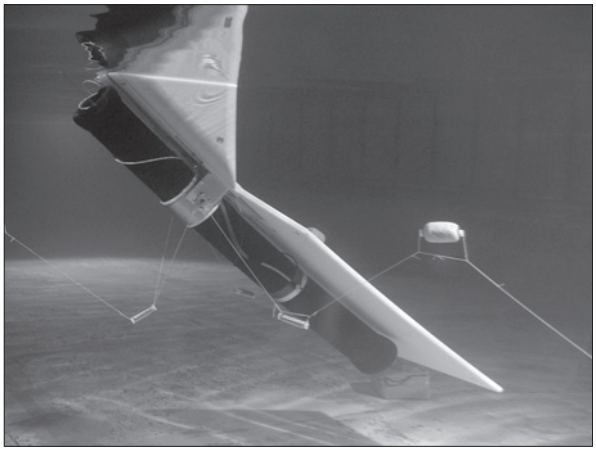

Figure 3: *A photograph of a free-floating model in the Edinburgh curved tank showing the moorings. A second fore mooring is obscured by the inertia plate.*

The models are being tested in the new Edinburgh 'curved' tank (Taylor, Rea, Rogers, 2003). Figure 3 shows a photograph of a model floating in the tank. The overall length of the tube was 1.1m. The low rate compliant moorings are there only to ensure that the model does not drift off station.

During the present experiments the piston was removed from the dynamometer tube. Measurements were made at different wave periods with first the dynamometer tube open at both ends to the water and then with the tube full of water but closed at both ends. These loosely correspond to the undamped and maximum damping

configurations of the dynamometer tube. If the dynamometer tube is appropriately sized with respect to the size of the rest of the model it is expected that these two conditions will lead to an observable difference between the motions. The motions were measured using a video tracking system from OptoMatrix Technology. Reflective markers are placed on the objects to be measured which are viewed from two cameras positioned so as to have different viewing angles. A ring of high intensity infrared light emitting diodes around the camera lens emit pulses which are reflected from the markers and then detected by the cameras. Using the information from the two cameras the three dimensional coordinates are calculated. Three rotational as well as the three translational coordinates can be calculated if the object being measured is marked with at least three markers. The cameras have a resolution of 60,000 by 45,000 pixels translating to a linear resolution of 0.03mm in the area of measurement. The worst case error in the present position measurements, combining the absolute resolution with calibration errors, was found to be +/- 0.1mm.

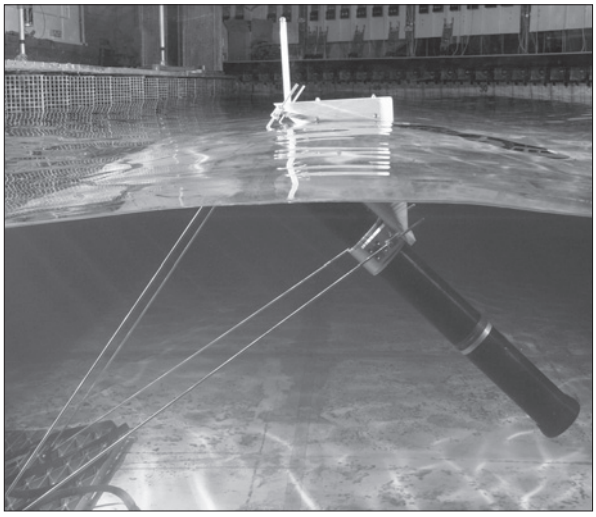

Figure 4: *A photograph of the constrained free-floating model showing the steel struts.*

To constrain the model to move at the desired angle whilst retaining the internal reaction system, four 8mm diameter steel struts, two at either side of the model, were used to tether the model to the tank floor. These had 'dry' rod end and flange spherical bearings at the bottom and top ends respectively, and were triangulated so that the model was free to move in an arc in the pitch direction, the radius of which was defined by the length of the steel rods. The model float angle was controlled by the respective lengths of the rods. The inertia plate was no longer needed to keep the model moving at the desired angle and was removed. The experimental set-up is shown in Figure 4, which shows the constrained free-floating model in the curved tank.

4. Numerical modelling

The computer prediction of the behaviour of marine structures in waves has now become reasonably accessible to the non-specialist.

The Wave Power Group at the University of Edinburgh is currently using WAMIT 6.03 for numerical modelling of wave power devices. This software has been developed under the direction of J.N. Newman and C H Lee from MIT and is widely used in the offshore industry. WAMIT uses a panel method for analysing hydrodynamic interactions with floating or submerged bodies, in the presence of surface waves. The flow is assumed to be ideal, free of separation or lifting effects and harmonic time dependence is adopted. The free surface and body-boundary conditions are linearised. Those assumptions mean that WAMIT can only properly model small wave conditions and that viscous effects and vortex shedding are neglected.

The geometry of the floating bodies can be input either analytically, using FORTRAN subroutines, or by a set of 'patches' approximating the body shape. In the later method, those patches can either be flat rectangular panels or smooth B-spline surfaces. The CAD package MultiSurf from AeroHydro was used to generate geometry description files compatible with WAMIT.

In order to build confidence with WAMIT, numerical predictions were compared with the historic tank measurements on Lin's constrained model (Salter 1998). In this configuration the floating model has only one degree of freedom: translation along the slope direction.

On Lin's model, the wave exciting force was measured by holding the model still in the tank while waves were sent at it, and recording the force required to keep the model in place. Figure 5 shows the comparison for the wave exciting force. The results are presented in the form of four graphs corresponding to the four different slope angles studied experimentally. The wave exciting force per metre wave height, also called the wave force coefficient, is plotted against wave period. The solid line shows the numerical prediction, the circles correspond to the experimental measurements for a 10mm wave height, and the crosses are the experimental points for a 50mm wave height. The numerical prediction shows a better match with the 10mm wave height points than with the 50mm ones. This is due to the linear hydrodynamic theory that WAMIT is based on. The higher the waves are, the less relevant the linear assumption is.

Further details on the comparison between experimental results and numerical predictions for this configuration can be found in Payne (2002).

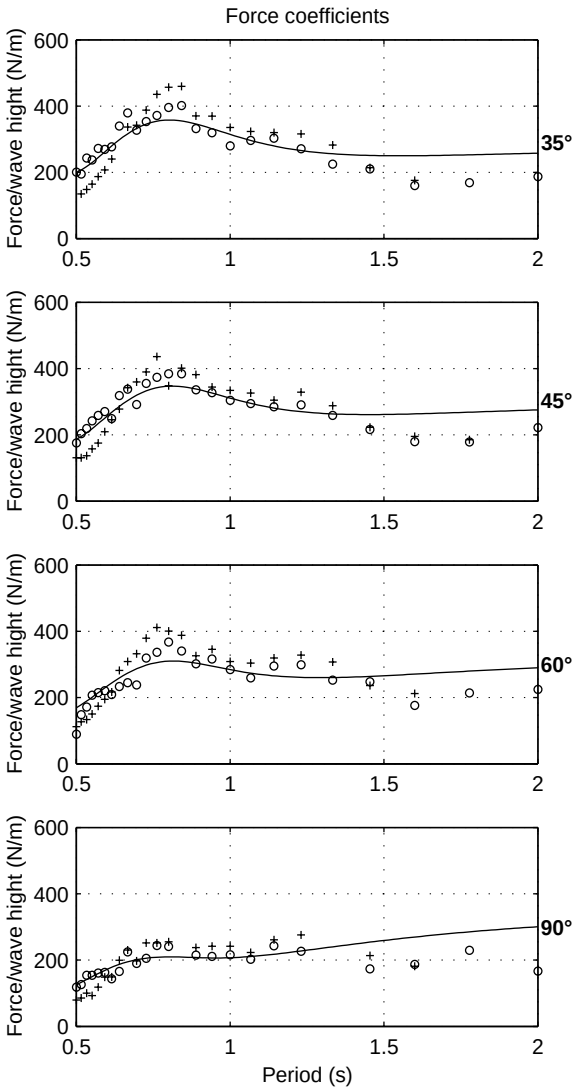

Figure 5: *Comparison between numerical predictions (solid lines) and experimental data for the wave exciting force. The crosses correspond to 50mm high waves and the circles to 10mm high waves.*

Following those encouraging results, the next stage was to predict the motions of the free floating model.

5. Results for the constrained free-floating model

Experimental results for the model held by the struts at a nominal still-water rest angle of 45° to the horizontal are shown in Figure 6. The figure shows the maximum excursion along the line of the prescribed arc, normalised by the wave amplitude and plotted against the wave period. Curves for the open and closed tubes are shown.

As noted earlier, the resonant frequency of a buoyant device is inversely proportional to the square root of the mass, thus it is expected that the natural period of a system will increase with mass. In addition, the amplitude of oscillation is proportional to the ratio of the reactive forces (buoyancy and inertia) to the damping force. Thus, if it is assumed that the buoyancy and damping are constant then an increase in mass will tend to increase the amplitude of oscillation. When the tube is closed and full of water this adds significant trapped mass to the system and accordingly both the period of resonance and its amplitude are higher for this configuration than with an open tube, the resonant period moving from approximately 1.6 to 1.82 seconds.

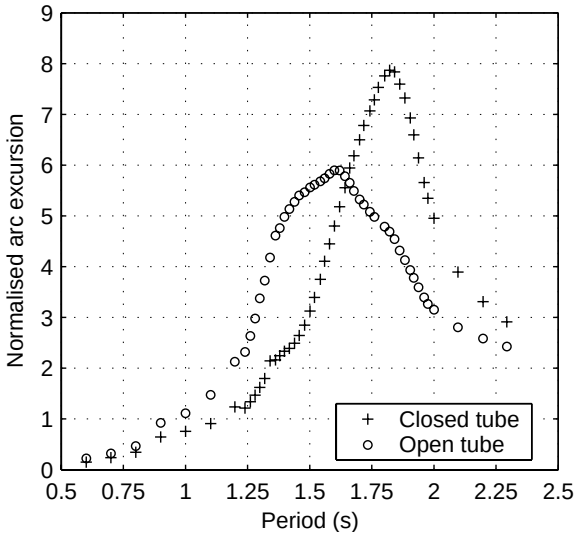

Figure 6: *Experimental data of the arc excursion of the constrained free-floating model for different wave periods. Data for an open dynamometer tube is compared with it closed.*

One of the fundamental principles of the sloped IPS buoy is that the mass of water in the tube acts as the reference for power take off. Therefore, in order for the piston to remain relatively fixed in space over the working range of periods, a significant resonance shift is required. These results show only a small difference between resonance periods. At the period when the model with the open tube is at resonance the model with the closed tube also has significant motions. This suggests that the dynamometer tube does not have the appropriate sizing with respect to the size of the rest of the model.

6. Results for the free floating model

All the measurements for the sloped IPS buoy reported thus far have been with the model constrained to move in the desired direction. The credibility of the concept is, however, dependent on the free floating device showing a strong tendency toward ‘slope movement’. To comprehend the movements in reality, or on video, is relatively easy, but to describe them in graphical or pictorial form is more difficult. Below is our attempt.

Figures 7 and 8 show experimental and numerical results of the motions of a free floating model, floating at a nominal rest angle of 35° to the horizontal. The figures

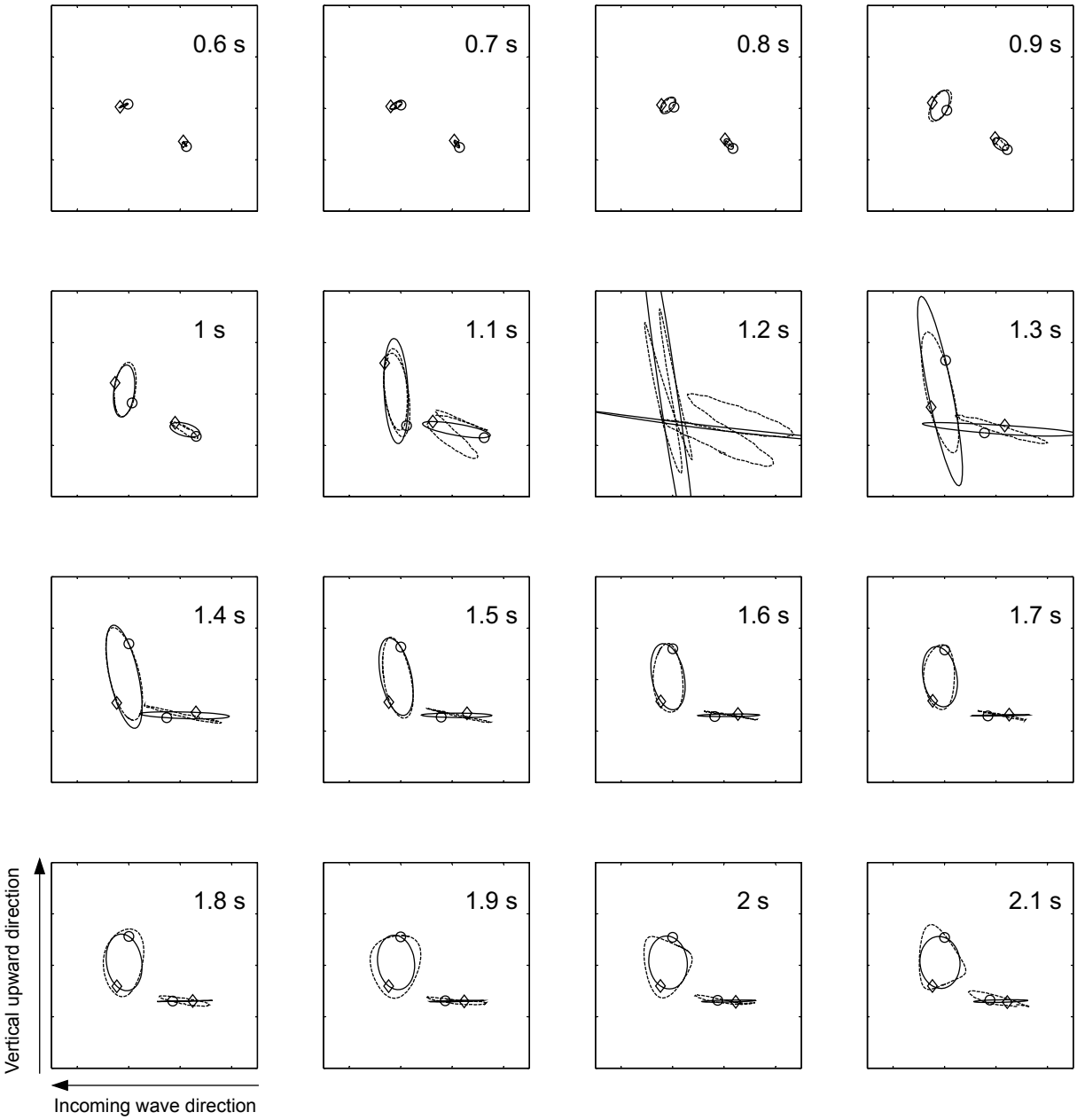

Figure 7: Open tube motion. *Traces of the motion path of both the top left hand corner of the model and the bottom of the plate with the tube open. Experimental data is shown by dashed line, numerical by solid line. The motions at the two points are separated by a distance which gives the correct angular separation of the centres of motions compared to the actual model. The circle indicates the point in the path corresponding to the crest of the incoming wave at the front of the float, the diamond to the trough.*

are respectively for the tube open and for the tube closed (but full of water). The model used a 20mm thick neutrally buoyant polyethylene inertia plate. It extended 0.9m from the end of the float and was 0.5m wide, but tapered in to the buoy diameter (see Figure 2). Each graph is a series of sub-plots showing the paths traced by both the top left corner of the model and the bottom of the plate, for different wave periods. The relative angular positions of the centres of the two paths is indicative of their relative spatial positions in reality, i.e. separated by the length of the model, but the actual paths have been scaled up to make them readable on the figure. This is because the size of the motions was small compared to the size of the model. The figure gives a qualitative rather than quantitative overview of the motion so no scales have been drawn. Each sub-plot is plotted on the same scale, however, so comparisons can be made. The experimental data is shown as dashed lines and the numerical as solid lines. The circle and the diamond show respectively the time of the crest and trough of the incident wave relative to the front of the float.

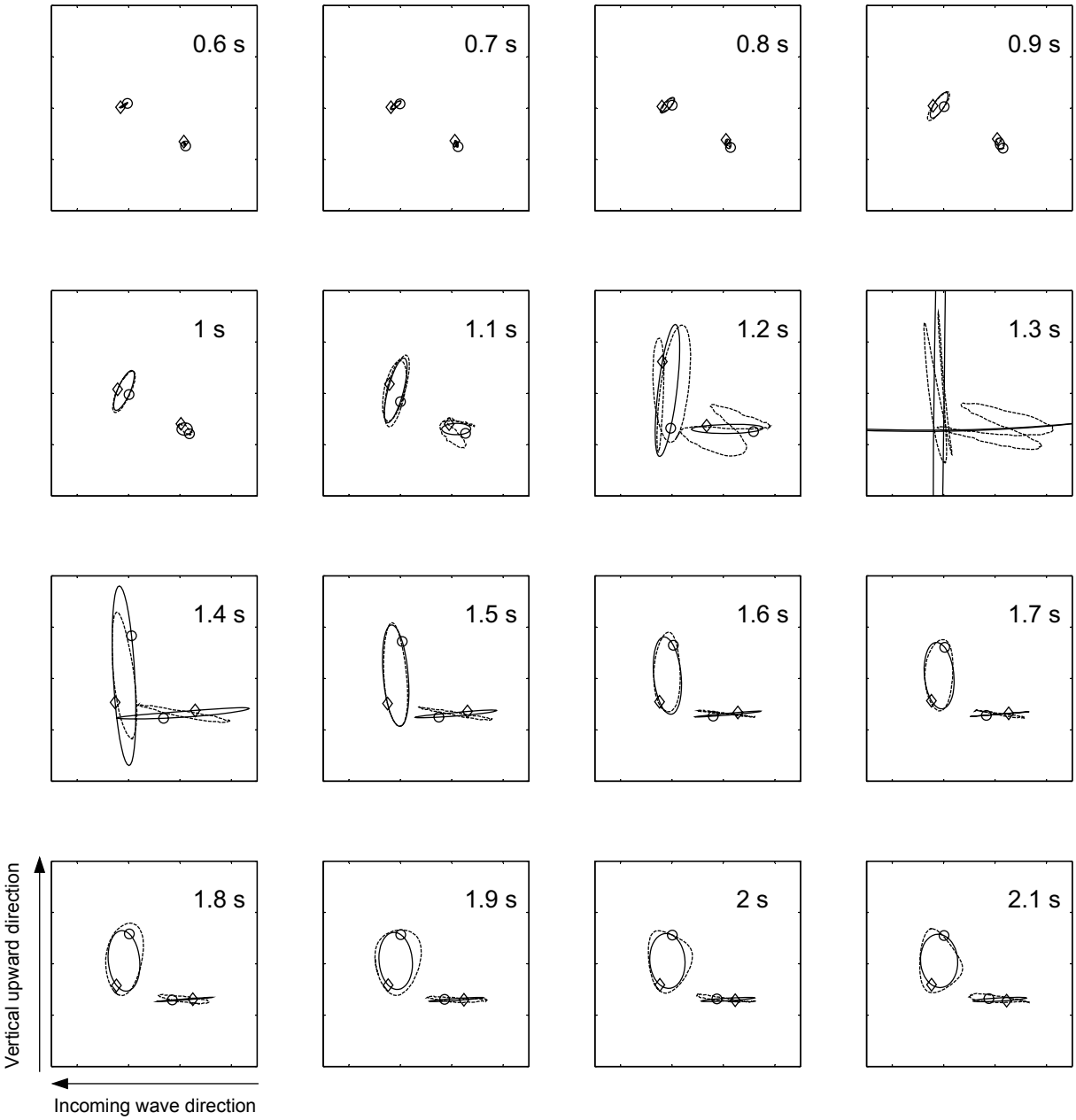

Figure 8: Closed tube motion. *Traces of the motion path of both the top left hand corner of the model and the bottom of the plate with the tube closed. Experimental data is shown by dashed line, numerical by solid line. The motions at the two points are separated by a distance which gives the correct angular separation of the centres of motions compared to the actual model. The circle indicates the point in the path corresponding to the crest of the incoming wave at the front of the float, the diamond to the trough.*

Figures 7 and 8 show clearly that the buoy is not moving simply along the direction of the inertia plate, as hoped for, but that the motion also incorporates a pitching movement. The top of the model moves around an irregular ellipsoid or 'potato' shaped path dominated by heave motions around the resonance periods of 1.2s and 1.3s for the open and closed tubes respectively. The bottom of the plate moves mostly in surge. Around resonance the experimental data scribes a butterfly shape. This corresponds to two wave cycles and is non-linear. The condition corresponds to an apparent resonance in roll and requires further investigation.

Although the desired motion of the model has not been achieved with this inertia plate, the comparison between experimental and numerical results is encouraging. This is shown quantitatively in Figures 9 and 10, plots of the normalised maximum displacements in heave and surge of the top left corner of the model with an open and a closed tube respectively. The experimental results are shown as circles and crosses and the numerical as dashed and solid lines for the heave and surge excursions respectively. There is very close agreement between experimental and numerical results except at heave

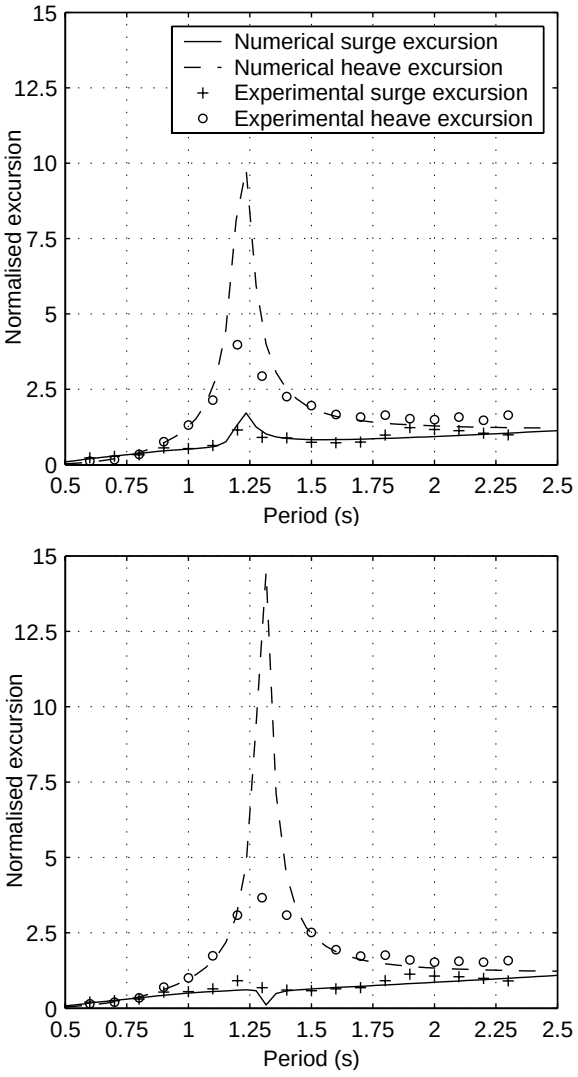

Figure 9&10: *Comparison between numerical and experimental data of the normalised heave and surge excursions of the top left hand corner of the model with an open tube (top) and closed one (bottom).*

resonance which occurres at periods of 1.2 and 1.3 seconds respectively, where the numerical results dramatically overestimate the motion. This is because vortex shedding and viscous effects, which play an important role in damping high amplitude motion, are not taken into account by WAMIT. The numerical simulation does, however, correctly predict the resonant period in both cases. As with the results of the constrained free-floating model, the small difference between the period of resonance of the two configurations seems to highlight the problem of the relative size of the power take off tube with respect to the inertia of the model.

The results presented above are for one specific model configuration with an arbitrary size and shape of inertia plate. The plate itself is relatively thick and, although it is neutrally buoyant, it has a large mass (43% of the mass of the model). A different size, shape or mass of plate could give different model motions. This is illustrated by Figure 11 which plots the normalised motion paths of the top of a model in which the polyethylene plate was replaced by a 2mm thick aluminium plate. Only the experimental results are shown. The dry weight of this plate was only a third of that of the polyethylene plate. The difference in mass meant that the model floated at 50° to the horizontal at rest. Because the inertia is significantly less than the previous results the resonant period has reduced, as has the amplitude of motion. In waves longer than the resonant period the motion is still the 'potato' shape, but at resonance and shorter periods the motion is much nearer to the direction of the slope angle.

Since the correlation between experimental and numerical results is so good, we now hope to exploit

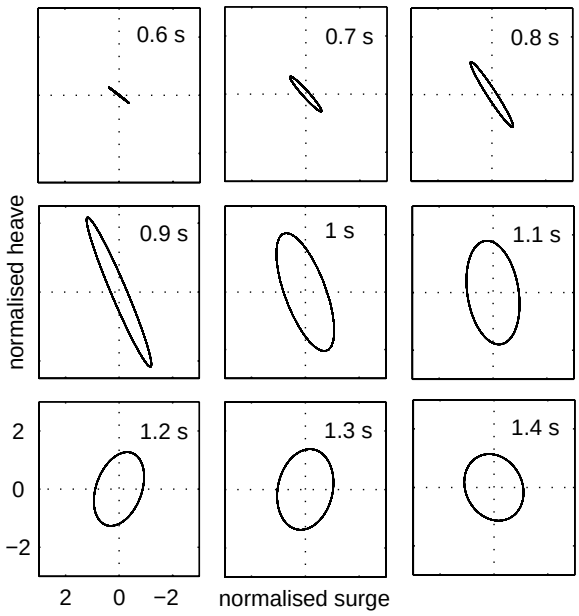

Figure 11: *Traces of the motion path at the top of the float of the model with an aluminium inertia plate.*

the potential of numerical simulation to explore the motions of different model configurations.

7. Conclusions

The results presented here highlight the challenges to be overcome before the realisation of the sloped IPS buoy as a wave power device. Relatively simple intermediate steps between the one dimensional fully constrained model and the three dimensional freely floating model have been described, and these have raised more questions than have been answered. The work has also highlighted the need for a combination of numerical and experimental approaches. The results from numerical modelling are encouraging.

Experiments with the constrained free-floating model demonstrate a tendency to move with a peak amplitude nearly eight times that of the incoming wave. However, the small motion differences between the open and closed power take-off cases must throw up doubts about its effectiveness in capturing energy from the model movement.

The concept of the sloped IPS buoy is dependent on its motions being close to the desired angle given by the plane of the inertia plate. The first free-floating model did not move in this way. The motions incorporated pitching as well as translations so the model tended to move in an ellipse dominated by heave at the top of the model and surge at the bottom. This was most pronounced around resonance. However, a second experiment with a lighter inertia plate showed how the motion is affected by the mass properties of the model. Comparisons between numerical and experimental results were found to be good, with the exception of the magnitude of the peak response at resonance.

Further work will exploit the time effectiveness and versatility of numerical modelling in exploring different model configurations to try to improve the action of the inertia plate in controlling model motion. Experimental work will continue alongside to allow ongoing verification and calibration. Research will also continue towards better understanding of the relative sizing of the component parts and therefore power capture of the model.

8. Acknowledgements

The authors would like to acknowledge the support of the DTI and EPSRC for the present work.

References

EC report. (1993). *Device Components and Materials*. Wave Energy Converters: Generic Technical Evaluation Study, Annex Report B2.

Fredrikson G. (1992). IPS wave power buoy mark IV. *Workshop on Wave energy R&D*, October, Cork (Ireland), pp.191-194.

Lin C. (1999). *Experimental studies of the hydrodynamic characteristics of a sloped wave energy device*. PhD Thesis, Department of Mechanical Engineering, University of Edinburgh, Edinburgh, U.K.

Payne G. (2002). Preliminary numerical simulations of the Sloped IPS Buoy. *Proceedings of the International Conference on Marine Renewable Energies (MAREC 2002)*, 11-12 September, Newcastle upon Tyne (U.K.), Institute of Marine Engineers, pp 79-88.

Pizer D. (1994). *Numerical Modeling of Wave Energy Absorbers*. DTI contract V/03/0172.

Salter S.H. (1992). The swinging mace. *Workshop on Wave energy R&D*, October, Cork (Ireland), pp.197-206.

Salter S.H. and Lin C. (1995). The sloped IPS wave energy converter. *Proceedings of the 2nd European Wave Power Conference*, 8-10 November, Lisbon (Portugal), pp.337-344.

Salter S.H. and Lin C. (1998). Wide Tank Efficiency Measurements on a Model of the Sloped IPS Buoy. *Proceedings of the 3rd European Wave Power Conference*, 30th September – 2nd October, Patras (Greece), Vol. 1, pp 200-206.

Taylor J.R.M. and Mackay I. (2001). The Design of an eddy current dynamometer for a free-floating sloped IPS buoy. *Proceedings of the International Conference on Marine Renewable Energies (MAREC 2001)*, 27-28 March, Newcastle upon Tyne (U.K.), Institute of Marine Engineers, pp 67-74.

Taylor J.R.M., Rea M. and Rogers D. (2003). The Edinburgh Curved Tank. *Proceedings of the 5th European Wave Power Conference*, 17-20 September, Cork (Ireland).